Mask collimation meets high-efficient data acquisition: a novel design of a low-dose-CT-Scanner for breast-imaging

Claudia Braun[1], Oleg Tischenko[1], Roswitha Giedl-Wagner[2], Helmut Schlattl[1], Christoph Hoeschen[1]

[1]*Research Unit Medical Radiation Physics and Diagnostics, Helmholtz Zentrum München, Neuherberg, Germany*

[2]*GFH GmbH, Laserbearbeitung und Mikropräzisionsfertigung, Deggendorf, Germany*

ABSTRACT

A novel designed x-ray CT scanning geometry is proposed. Composed of a specially designed tungsten collimation mask and a flat panel detector, which is placed inside the mask, this scanning geometry provides high efficient data acquisition allowing dose reduction potential by a factor of two.

In recent years a first prototype of the CTDOR geometry (CT with Dual Optimal Reading) has been evaluated. It consisted of a discontinuous ring of detectors fixated on X-Ray absorbing material. The source and an outer detector were mounted on a gantry rotating around the inner static detector and the patient. Despite many drawbacks, resulting images have shown promising potential of dual reading. Based on those results, the present work presents further development and improvement of the recommended scanner geometry. The main idea consists of collimating the X-ray beam through a specially designed shielding mask thereby reducing radiation dose and structuring data without compromising image quality. An especially developed high precision laser-beam cutting process assures an accurate mask crafting with tungsten shielding and window sizes of 300µm.

Additionally, simulation data were obtained with Monte Carlo calculations to test the dose reduction potential of the scanning device. Retaining advantages of the CTDOR geometry such as 3D-capability, built-in capacity of scatter correction and radiation structuring, a high-precision manufactured collimation mask of novel designed CT-scanner enables high resolution images for breast-imaging in low energy ranges.

1. Introduction

Digital x-ray mammography is the today's standard approach for early and reliable detection of breast carcinoma. However, there is an intense debate on its sensitivity and specificity regarding superimposition of anatomical structures. This still remains a challenge.

Consequently, different alternative approaches are of great interest. Among these, Computed Tomography (CT) provides a promising technology. The proclaimed imaging procedure should meet the demands of breast imaging [1], i.e. 3-D-capability, good soft-tissue differentiation, high spatial resolution and low patient dose. Although it would be justified to increase the dose to the patient if there is a valid indication such as higher diagnostic information for cases of suspected breast cancer. Nevertheless it is worthwhile to stay within the dose limit frame imposed or screening, where the benefit-to-risk-ratio is very high [2]. Furthermore the ICRP recommends following ALARA principle, i.e. patient dose has to be kept "As Low As reasonably Achievable" [3].

Medical Imaging 2013: Physics of Medical Imaging, edited by Robert M. Nishikawa, Bruce R. Whiting, Christoph Hoeschen, Proc. of SPIE Vol. 8668, 86684H · © 2013 SPIE · CCC code: 1605-7422/13/$18 · doi: 10.1117/12.2007832

In this context, a new type of scanner geometry has been presented at SPIE Medical Imaging 2006 [4] and was reported to have dose reduction potential by a factor of two, without compromising image quality [4,5]. This geometry is based on the principle of CTDOR (CT with dual Optimal Reading). Two groups of detectors are collecting collimated x-rays in order to yield two complementary sets of data. The collimation type (Fig.1B) results in parallel beams that are distributed according to the zeros of Chebyshev polynomials in each projection [4]. Such a distribution is exactly what is needed in the reconstruction algorithm OPED (Orthogonal Polynomial Expansion on Disc) proposed in 2006 [4]. Moreover scatter radiation can be obtained without any additional effort or exposure and hence entails a built-in capacity for scatter correction [9].

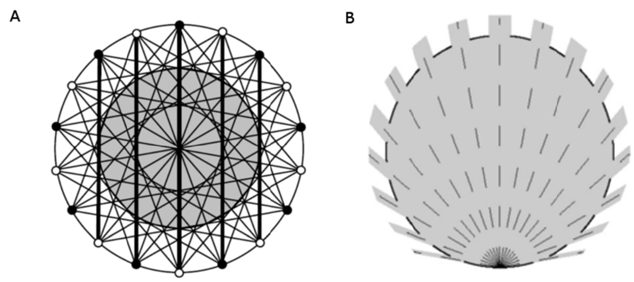

Fig.1: Parallel beam distribution according to zeros of Chebyshev polynomials (A) and suitable collimation type (B) [4]

A first prototype of CTDOR has already been built [5]. The first subset of data is collected by ring center facing detectors, which were mounted on structured lead shielding, whereas the gantry detector, which was placed outside the ring, gathers the second set of data. Together with mask detectors, 197 collimators with size of 2.5mm built up a discontinuous absorbing ring, permitting x-rays passing through 3mm holes as shown in Fig.2.

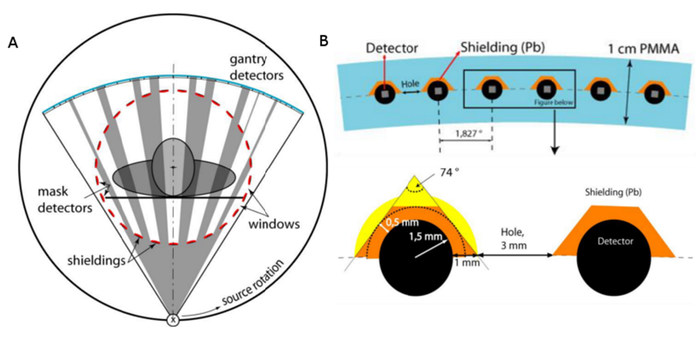

Fig.2: Schematic view of CTDOR (CT with dual Optimal Reading) prototype (A) and demontrator's mask design (B)

Although images presented by de las Heras et al., 2008 [6] and Brunner et al., 2012 [8] have shown promising potential of dual reading, this prototype has some drawbacks: first, mask and arc data are difficult to match due to the different detector types. The size of mask detectors, in addition, defines the maximum number of views and results in a sparse count of 394 for the demonstrator. Due to its construction, the proposed scanner is only capable of 2-D. Furthermore, irregular window sizes have led to incorrect data readout.

In order to overcome these drawbacks a novel design of CT scanning geometry using the principle of CTDOR data acquisition is being developed. This design is especially made up for breast-CT in low energy ranges.

2. New Scanner geometry

For high resolution capability we designed a collimation mask that is built up by shielding rods with diagonal sizes of 300µm. The collimators are, in cross section, shaped as quadrature structures with their diagonals pointing towards the ring center. Hence, each radiation absorbing element admits radiation beam structuring and efficient data collection, while maintaining a maximum of radiation protection.

Similar to 3rd generation of CT scanners, source and detector are co-rotating around the object, whereupon the mask collimators remain stationary. Traversing radiation is collected by a flat-panel detector, whose pixel size is about one order lower than the size of absorbing elements and windows respectively. The detector is located within the mask and can therefore acquire the two independent subsets of data. Hence, the same amount of information as acquired by CTDOR can be obtained here without any need of matching two types of detector sampling.

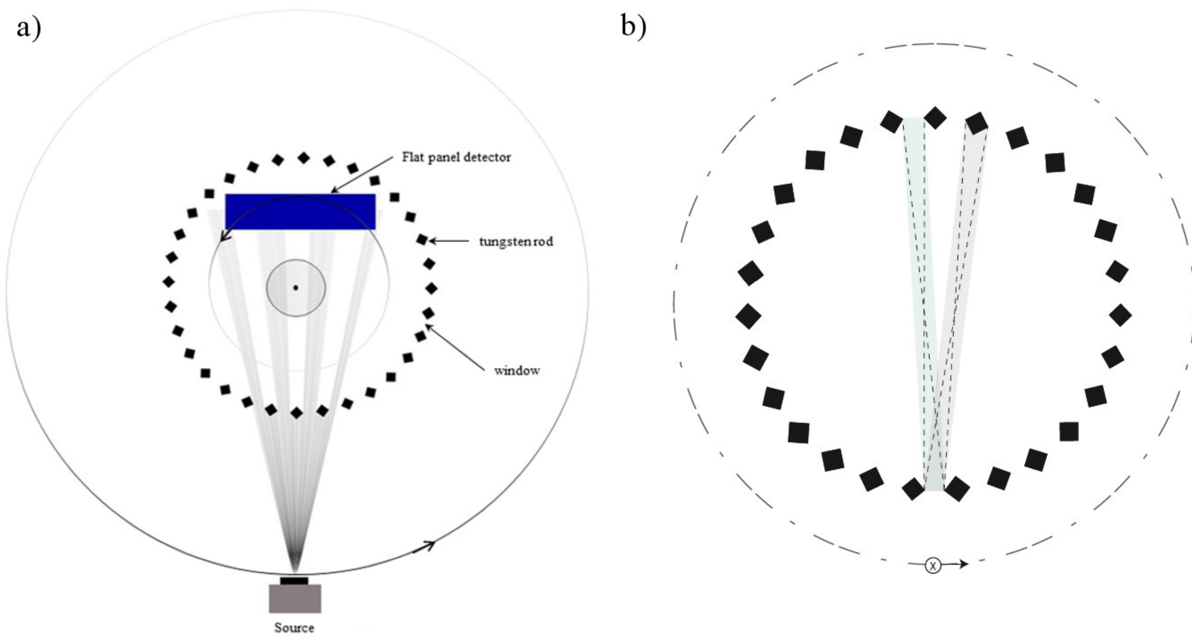

Fig.3: Sketch of the new scanning principle. A flat panel detector is placed inside a special designed tungsten mask. X-ray tube and detector are rotating around the object in a similar manner yielding an interlaced grid of radiation (a). Chords are configured to collect two sub-sets of data (b)

With a given angle to the central beam of the projection each ray contributes to a certain parallel beam. Suggesting windows and shielding elements as points uniformly distributed over the circle, where the number of windows is denominated as N, sub-sets of data are made up by the configuration of the chords connecting two N points. For each of subsets, one example of a chord is pictured in Fig.3b. After reordering the data to parallel geometry with sinusoidal lateral sampling, one obtains the matrix $P := \{p(i,j) | i=0,\ldots,N-1, j=0,\ldots,N-1\}$, where $p(i,j) = 0$ if $i+j$ is even. Hence, the data is defined on an interlaced grid. It is known [12] that the data defined on such a grid are equivalent to the data defined on the full rectangular grid (i.e. $p(i,j)$ with even $i+j$ are known as well). The missing data, $p(i,j)$ with $i+j$ being odd, is recovered following the method described in Ref.13 and one obtains the completed matrix of parallel data that can be reconstructed with OPED [11].

3. Methods

3.1. Mask design

Surface and edge quality as well as precision-engineered tolerances in the maximum range of ±20µm are essential factors for implementation of good collimation performance and high resolution achievement. Thus, a special crafting process is needed to get the desired composition of shielding elements. In doing so, low cost, size dimensions and stability of the desired 3D-structure has to be achieved as well as the absorption coefficient, brittleness and molar heat capacity of the utilized material. The processing method has been developed in collaboration with GFH Deggendorf, using the high precision laser beam system GL5.evo and tungsten as the shielding mask material.

The laser processing itself is currently under development and it would be executed in two steps. In the first step, the laser cuts gaps with an incident angle of 45 degrees. After pivoting the tungsten segment around 90 degrees, versus cuts are executed providing the desired X-pattern of the collimation mask. In each case of step an optical measurement system enables an accurate appointment of the laser beam starting position.

This cutting process would be accomplished by a picosecond pulsed laser (1030nm, 200kHz, 50W). For first testing tungsten was treated with a rotating beam, laser galvo-scanner (Fig.4Cii) (power=50%; feed rate =70m/min; radius of rotation=0.050mm, 1000requests; rectangular path). The area of work was cooled by a Crossjet (1.5bar; air).

In order to achieve higher precision, the laser beam system GL5.evo (Fig.4C) was expanded with the module GL.Optifix (Fig.4Ci). Here, tungsten sheets are cut with axial movement and a fixed optic. To get the desired height of remaining shieldings at 8mm, GL.Optifix has to be modified. Similarly as for galvo scanning, the laser beam rotates at 6000rpm. The diameter of rotation was opted for 200µm to attain a cutting width of 210µm. Executed at two angles of incidence, sizes of 300µm turned out both for collimator width as well as for intermediate distances.

Cut by laser beams, crafted tungsten sheets were viewed under a light microscope and evaluated in terms of distance variations, edge quality and structural equality.

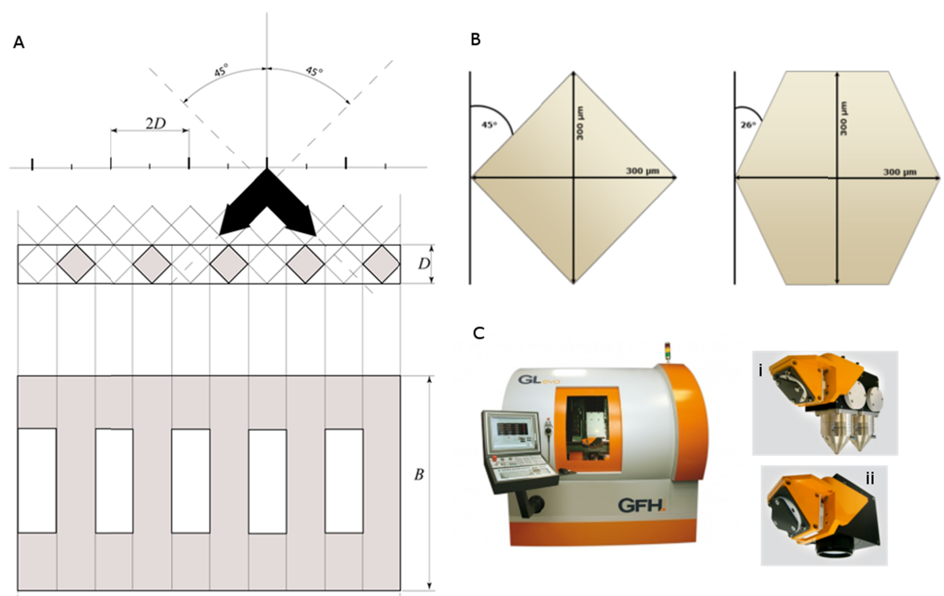

Fig.4: Laser cutting process. The proposed procedure is accomplished by pulsed laser beam treating system GL5.evo (C). Due to crafting results the angle of incidence has further been reduced to 26°

3.2. Simulations studies

Since high density material such as tungsten is more difficult to be cut by laser beam at an oblique angle of incidence, Monte Carlo method have been used to evaluate different collimator geometries. Two different simulation studies have been performed using the Geant4 toolkit.

In each case the energy spectrum corresponds to a tungsten anode spectrum at 50kVp with a filtration of 0.1mm Cu and 0.1mmAl. The detector is both assumed to be linear responding to deposited energy.

In a first study, the attenuation profile as well as the dose reduction was simulated for cutting angles 0° and 45° to reconsider the necessity of collimator geometry. Neglecting low portion of scatter radiation (as can be seen later) caused by shielding mask, only primaries are collected after traversing the tungsten mask. The source-detector distance (103mm) is selected to be as far as needed to get correct pixel read-out considering tolerance for tungsten mask laser crafting in the range of ±20µm. Further parameters used in this evaluation are depicted in Table 1.

In a second study, the attenuation performance of one single collimator has been performed. Therefore three different types of collimator geometry are considered (see Fig.5). Apart from primary radiation, Compton and Rayleigh scatter as well as electrons are taken into account. Parameters for this attenuation performance studies are quoted in Table 2.

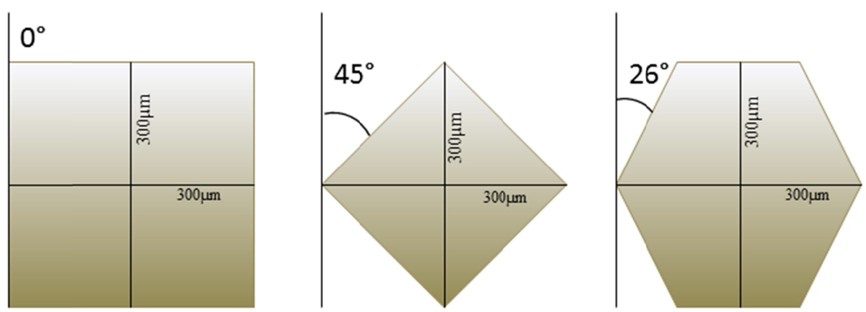

Fig.5: Three different types of collimator geometry resulting from different laser cutting angles (cross section view)

Table 1: Parameters set for attenuation profile and the dose reduction calculations

Fan angle	8.23°
Pixel size	0.0748mm
Focal spot size	0.070mm
Source to detector distance	397.382mm
Source to mask distance	103.0mm
Number of collimators	1800
Number of pixels	1536
Number of views	2
Number of photons	100000000

Table 2: Parameters set for attenuation performance studies of collimator geometry

Cone angle	14.8°
Pixel size	0.0748mm
Focal spot size	0.070mm
Source to detector distance	324.382mm
Source to collimator distance	40.0mm
Number of collimators	1
Number of pixels	100x100
Number of views	1
Number of photons	10000000

The yielding values of transmitting particles, the dose reduction factor can be estimated by following equation:

$$Dose\ reduction\ factor = \frac{total\ beam\ energy}{permitted\ energy}$$

4. Results and Discussion

The attenuation profile of collimator geometry has been simulated for an incident angle of 0° and 45° to point out the necessity of the proposed mask collimator design . Fig.6 shows an example of the intensity profiles for a single view. It can be seen, that, the shielding elements of the tungsten form a uniform distribution of intensity chords. For both types of geometry, the collimation mask offers the same attenuation performance in the middle of the detector region (not shown here). Contrary to that, in outer detector regions (see Fig.7), the data output of 45° cut shielding rods is higher than the data output of zero cutting angle. At the same time, the dose reduction factor was estimated to be similar for both geometry variations at a value of about 2.2 (see Table 3 and Table 4). Thus, in order to get maximum data output, maintaining dose reduction at highest possible level, one has to decide for rotated quadrature structures, i.e. for a laser beam cutting incident angle of 45°.

However, the penumbra regions of the proposed collimator design are significantly wider than the quadrature shaped shieldings that result from cutting angle of 0°. Therefore a second simulation study was performed to compare another type of collimator geometry to the proposed one (see Fig.5). Apart from primary and attenuated radiation, Compton scatter as well as Rayleigh scatter had been taken into account.

All collimator geometries produce low portion of scatter radiation (results are not shown in here). Fig.8 depicts detector images of the three kinds of shielding elements yielded by traversing primary particles. Compared to the laser cutting angle of 45°, penumbra regions of hexagonal design are significantly improved (Fig.8). In order to maintain maximum output of data, thereby ensuring perpetuation of x-ray absorbing, the minimum incident angle of laser cutting (Fig.5) has to be calculated by the following equation:

$$\beta = \sin^{-1}\left(\frac{R}{r}\right)$$

where r is denoted as the mask radius and R as half of maximum FOV size. In our case, β is determined to be at minimum 26°. Changing the cutting angle even more, i.e. to 16° (not shown here), attenuation performance is deteriorating again.

Table 3: Dose reduction estimation for zero set laser cutting angle

	View 1	View 2
Source/detector rotation	0.0°	0.1°
Total beam energy [keV]	$2.74972 \cdot 10^8$	$2.75030 \cdot 10^8$
permitted energy [keV]	$1.21073 \cdot 10^8$	$1.22213 \cdot 10^8$
Dose reduction factor	2.2711	2.2504
Estimated reduction factor	2.2606	

Table 4: Dose reduction estimation for proposed scanner mask design

	View 1	View 2
Source/detector rotation	0.0°	0.1°
Total beam energy [keV]	$2.74985 \cdot 10^8$	$2.74918 \cdot 10^8$
permitted energy [keV]	$1.49170 \cdot 10^8$	$1.10903 \cdot 10^8$
Dose reduction factor	1.8434	2.4789
Estimated reduction factor	2.1611	

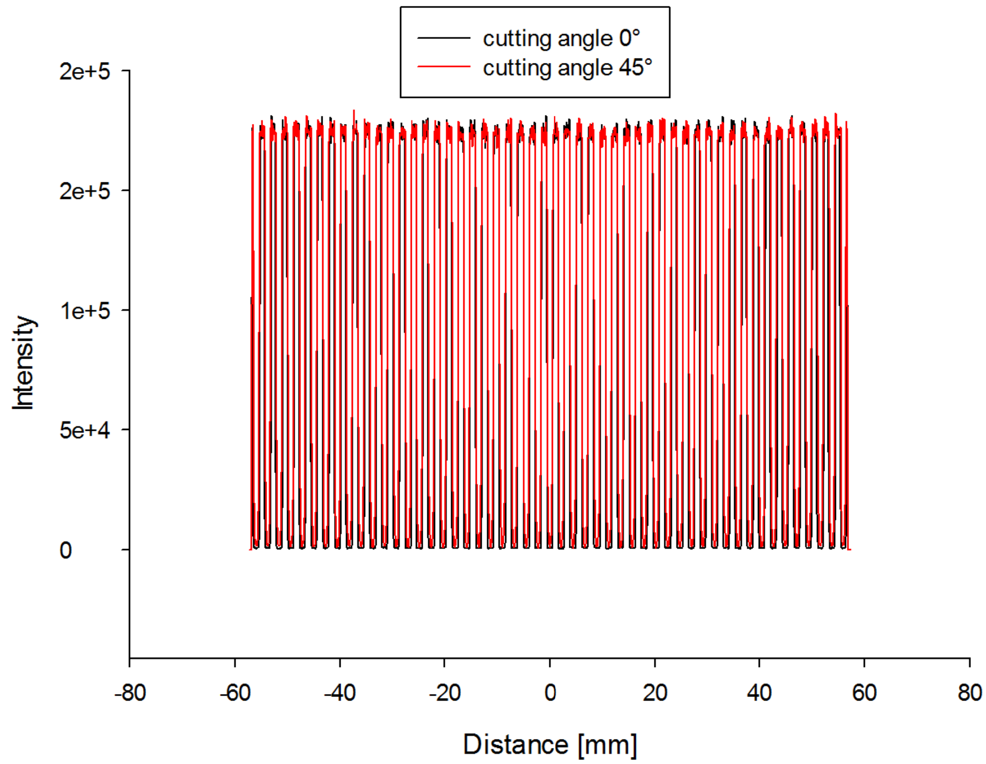

Fig.4: Intensity profile of simulated tungsten mask at source position of 0°

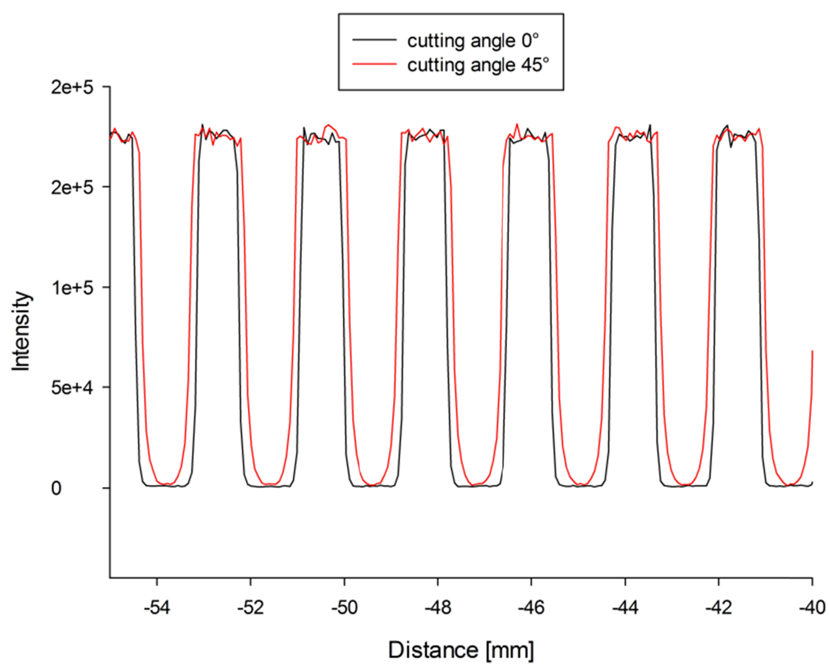

Fig. 5: Magnified intensity profile in outer detector regions.

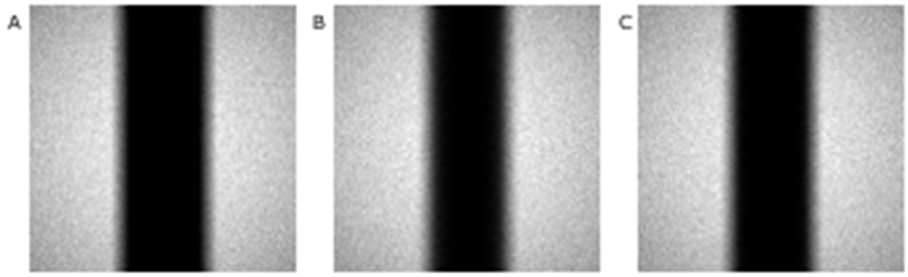

Fig.6: Simulated images of three different types of collimation geometry: cutting angle 0° (A), 45° (B) and 26° (C)

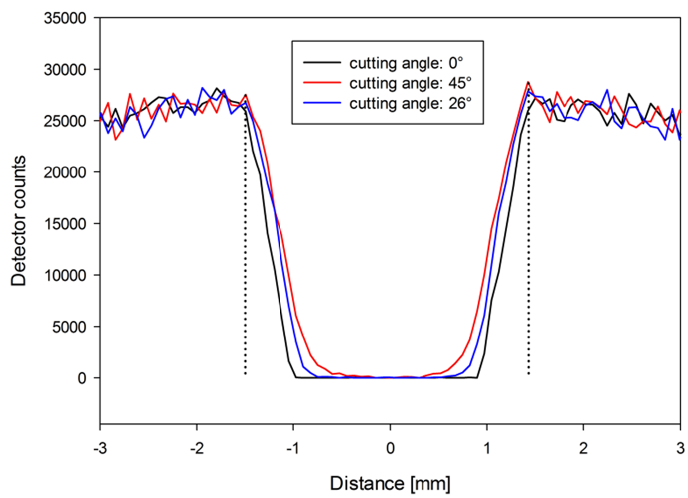

Fig.7: Penumbra regions of three different collimator designs

The proposed laser cutting process generally works. However, the heat impact on a single, 8mm high rod turned out to be too high and thus deformed the collimator mask (Fig.10A). Further on small bars remain between the collimators (Fig.10B). This leads to an unsatisfactory result that could be improved in different ways.

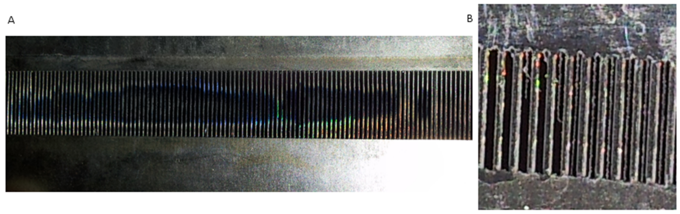

Fig.8: Mask deformation as consequence of too high impact on tungsten collimators (A). Small bars of mask material remain after proposed laser cutting process (B)

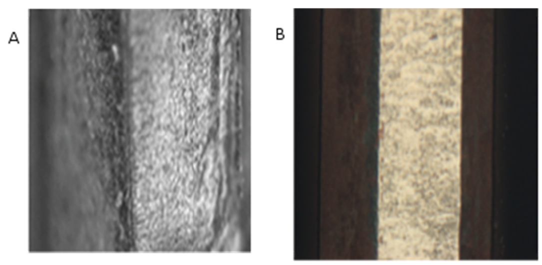

Fig.9: Light microscopy images of edge quality for quadrature shaped collimators (A) and hexagonal design (B)

The height of the tungsten rods has been reduced to 4mm. Because of improved attenuation performance as seen in the simulation studies and also because of increased stability, the collimator geometry (in cross-section) has been changed from quadrate to a hexagonal design. Several tests of modified laser cutting process have further been performed. The problem of heat impact could be eliminated in this way because of higher collimator thickness in general (see Fig.5). Edge precision could further be improved (Fig.10). Due to lower incident angle there is also no need to apply an extra processing step to cut out the small bars. In the whole clamping construction, at last, a final version of crafted tungsten mask can be seen in Fig.11.

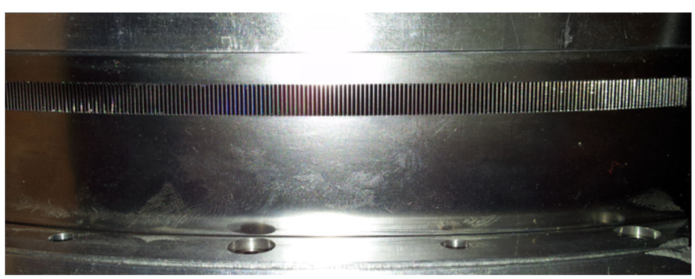

Fig.10: Example of crafted tungsten mask in the final clamping construction

5. Conclusion and Outlook

A novel design of CT scanning geometry is recommended. An accurate laser processing technique has been evaluated to ensure high quality data-readout with an estimated dose reduction factor of two. Hexagonal shielding geometry also reduces the width of penumbra regions allowing high efficient data collection at maximum attenuation.

Due to its construction principles, the proposed scanner maintains the advantages of the CTDOR scanning principle while avoiding its drawbacks by limited resolution and the use of separate detectors. The efficient data collection and data structuring in combination with the reconstruction algorithm OPED could yield images of high resolution. The intrinsic scatter-correction potential will prove valuable when the system would be operating in 3D mode. The proposed scanner geometry may therefore provide comprehensive diagnostic assessment of microcalcifications and soft-tissue structure at one half reduced dose levels.

A scanner prototype is currently assembled and is expected to give evidence of high resolution possibility, scatter correction potential and helical imaging mode at low-dose level.

REFERENCES

[1] Kalender, W.A., [Computed Tomography], Publicis Publishing, Erlangen, (2011).

[2] Yaffe, M.J. and Mainprize, J.G.,"Risk of radiation-induced breast cancer from mammographic screening," Radiology 258, 98-105 (2001).

[3] ICRP, “Managing patient dose in multi-detector computed tomography,” Annals of the ICRP 103 (2007).

[4] Tischenko, O., Xu, Y. and Hoeschen, C., "A new scanning device in CT with dose reduction potential," Proc. SPIE 6142, 61422L (2006).

[5] de las Heras, H., Tischenko, O., Schlattl, H., Xu, Y. and Hoeschen, C., "Modelling and testing of a non-standard scanning device with dose reduction potential," Proc. SPIE 6510, 6510R (2007)

[6] de las Heras, H., Tischenko, O., Renger, B., Xu, Y. and Hoeschen, C., "Experimental proof of an idea for a CT-scanner with dose reduction potential," Proc. SPIE 6913, 691307 (2008).

[7] de las Heras, H., Tischenko, O., Schlattl, H., Xu, Y. and Hoeschen, C., "Dose reduction potential of the scanning geometry CT D'OR: a simulation study," Proc. SPIE 7258, 72585R (2009).

[8] Brunner, C.C., Tischenko, O., de las Heras, H., Benger, B., Schlattl, H. and Hoeschen, C., "The CTDOR geometry: An optimized data treatment to demonstrate ist potential," Proc. SPIE, (2009).

[9] Schlattl, H., and Hoeschen, C., "The built-in capacity of CT D’OR’s static ring for scatter correction," Proc. SPIE 6913, 691352 (2008).

[10] Natterer, F., "Sampling in fan beam tomography," SIAM J. Appl. Math 53 No. 2, 358-380 (1993).

[11] Xu, Y., "A new approach to the reconstruction algorithm for Radon data," Advances in Applied Mathematics 36, 388-420 (2006)

[12] Rattey, P.A. and Lindgren, A.G., "Sampling the 2-D Radon transform," IEEE Trans. Acoust. Speech Signal Processing, ASSP-29, 994-1002 (1981).

[13] Fadriani, A. and Ritman, E.L., "High Resolution computed tomography from efficient sampling," Inverse Problems 16, 635-650 (2000).